Critical roles of Fe²⁺/Fe³⁺ in manipulating permanganate reactivity with zero-valent iron towards enhanced arsenite removal

Tianying Chang[a,b], Yue Wang[a,b], Zhengchao Zhang[a,b], Tingyi Liu[a,b,c],*

[a]*Tianjin Key Laboratory of Water Resources and Environment, Tianjin Normal University, Tianjin 300387, China,*
Tel./Fax: +86-22-2376-6557; emails: liutingyi@tjnu.edu.cn (T. Liu), tiangyingchang@163.com/tianyingchang0412@163.com (T. Chang),
wy13502181683@163.com (Y. Wang), 13116156253@163.com (Z. Zhang)
[b]*School of Geographic and Environmental Sciences, Tianjin Normal University, Tianjin 300387, China*
[c]*International Center for Balanced Land Use (ICBLU), The University of Newcastle, Callaghan, NSW 2308, Australia*

ABSTRACT

Due to the higher toxicity and great threat to environmental safety and human health, the remediation of As(III) from wastewater attracts more and more attentions. The introduction of Fe²⁺ and Fe³⁺ into potassium permanganate (PP)-zero-valent iron (ZVI) system was used to rapidly and effectively remove arsenic (III) from wastewater. PP-ZVI system was rapidly activated by Fe²⁺ but Fe³⁺ in a slow way. The high removal efficiency of As(III) in Fe²⁺-PP-ZVI system was obtained at pH_{ini} 1–9. The removal of As(III) by Fe²⁺-PP-ZVI system can be well described by the pseudo-second-order kinetic expression. The results of scanning electron micrographs (SEM) showed that the quickly enhanced corrosion of ZVI surface caused the different morphologies of ZVI surface. ZVI acted as a resource of Fe²⁺ for the activated generation of •OH radicals, which oxidized As(III) to As(V). High-resolution X-ray photoelectron spectrometer (HR-XPS) proved that $MnFe_2O_4$, MnO_2 and MnO were formed, which controlled the generation of hydroxyl radical (•OH). Most of As(III) was oxidized to As(V) but a very small proportion was reduced to As(0) during the removal process. The Fe²⁺-PP-ZVI system may provide an effective and new technology for the efficient and fast remediation of heavy metals from wastewater.

Keywords: PP-ZVI system; Hydroxyl radical (•OH); Arsenic(III); Heavy metals

1. Introduction

Arsenic, as one of the most toxic pollutants, usually exists in aquatic systems as inorganic forms ((As(V)) and (As(III)) [1]. Moreover, As(III) has attracted more attentions because it is more mobile and poisonous than As(V) [2]. With the development of natural processes and anthropogenic activities [3,4], arsenic pollution is a serious threat to human health and aquatic ecosystems [5]. According to statistics, there are about 150 million people, who are living in the arsenic-contaminated environment [3]. Therefore, the removal of As(III) from wastewater has become a global problem to be solved [1,3]. As we all known, As(V) is more inclined to be adsorbed on the surface by ferric oxydroxides than As(III), so an oxidant is usually introduced into the process of As(III) removal [1,3].

In recent years, zero-valent iron (ZVI) has been widely used to degrade various organic pollutants and heavy metals [6–8]. Nevertheless, the formation of passivation layers on the surface during the reaction led to a decrease in ZVI reactivity, which extremely limited the development of ZVI in the field of water environment treatment [9]. To overcome the problems, a series of strategies to significantly activate ZVI to degrade and remove various contaminants

* Corresponding author.

were proposed [10,11], especially the advanced oxidation processes [12]. It was mainly added chemical oxidants such as permanganate and H_2O_2 to the ZVI-based system to generate strong radical oxidants and improve their decontamination capability [12,13]. It was reported that Fe(II) and Fe(III) played important roles in arsenic removal because they could catalyze the production of $^{\bullet}OH$ via Fenton-like reactions [4,10,14]. In addition, arsenic(III) was rapidly oxidized and adsorbed to magnetite and ferrihydrite surfaces due to Fe^{2+} and oxidant [4].

Furthermore, permanganate (MnO_4^-) is extensively developed as a 'green' strong oxidant because it is not only have moderate price and easy storage but also high activity without producing harmful by-products during the reaction [15]. In recent years, it is popular to apply permanganate to remove organic and inorganic pollutants [8,16]. The reactivity of ZVI can be strongly activated by permanganate, which remarkably enhance heavy metals (<1 mg L^{-1}) and nitrate (NO_3^-–N = 14 mg L^{-1}) removal from wastewater [9,17].

Consequently, potassium permanganate (PP) was obviously activated by Fe^{2+} through producing $^{\bullet}OH$ radicals, leading to the rapid removal of various contaminants [12]. However, the rapid consumption of Fe^{2+} influenced the removal capacity of target pollutants using this system, so it was necessary to introduce ZVI as source of Fe^{2+}. The introduction of Fe^{2+} and Fe^{3+} into PP-ZVI system was little investigated. In addition, it was unclear that what the mechanism of the manipulation or activation of the reactivity of PP-ZVI system happened by Fe^{2+} and Fe^{3+}. Herein, we added Fe^{2+} and Fe^{3+} to the PP-ZVI system to further reveal the enhancement mechanism of the removal of As(III) in this system. Our study aims to: (1) discuss the enhancement or activation mechanism of Fe^{2+} and Fe^{3+} on the As(III) removal in the PP-ZVI system, (2) compare the effect of Fe^{2+} and PP on As(III) remediation in such ZVI system, and (3) investigate the surface characterization of ZVI in such system using microscopic and spectroscopic technology to reveal the removal mechanism of As(III) in such ZVI-based system.

2. Experimental section

2.1. Chemicals and reagents

All the chemical reagents had reached or even surpassed to the analytical grade purity. Ferric trichloride (GR grade) and ferrous sulfate (GR grade) were provided by Fuchen Chemical Reagent Manufactory (Tianjin, China). Potassium permanganate (PP) ($KMnO_4$, GR grade) was obtained from Spain Scharlau Company. ZVI power (>99.0%) used in the study was purchased from Tianjin Guangfu Technology Development Co. Ltd. 1 g L^{-1} $NaAsO_2$ (AR grade) standard solution was purchased from National Centre for Certified Reference Materials (Beijing, China). Deionized water was supplied by Tianjin No. 1 Chemical Reagent Factory.

2.2. Batch experiments

Batch experiments researched the removal mechanism of As(III) in PP-ZVI system. The specific experimental operation was as follows: initially, wastewater for the experiment was pre-made by continuously diluting the As(III) standard solution with deionized water to make As(III) concentration

reach 20 mg L^{-1}. Then, a certain amount of PP, ZVI and ferric trichloride or ferrous sulfate were weighed and placed in a polyethylene bottle. Subsequently, the prepared As(III) solution was poured into a polyethylene bottle and placed on a water bath constant temperature oscillator for total 1 h at room temperature. During the reaction, using a 2 mL dispensable injector to sample the reaction solution at a specific time intervals (0.5, 1, 2, 5, 10, 20, 30 and 60 min) and filtering other impurities through a 0.45 μm filter membrane. Finally, the liquid sample was diluted to a concentration for further testing.

Add a certain amounts of ZVI, Fe^{2+} and Fe^{3+} to the reaction system to determine their role in the study. Change the dosage of Fe^{2+} or PP under the same conditions to reveal the enhancement or activation effect of As(III) removal.

The initial pH of the As(III) solutions was adjusted with dilute HCl or NaOH to determine the range of 1–9. In addition, there was no buffer solution added to control pH during the reaction.

2.3. Characterization and analytical methods

The concentration of Fe(II) was measured by 1,10-phenanthroline colorimetric method at 510 nm [18,19]. The concentrations of total arsenic, iron and manganese in reaction system were measured by inductively coupled plasma-mass spectrometry (ICP-MS, Elan-9000, PE) [20].

The elemental composition and chemical state of ZVI after reacting with As(III) solution was investigated by HR-XPS (PHI 5000 Versa Probe) at 46.95 eV. The XPS results were analyzed by Origin 9.0 software. The surface morphology of ZVI in different reaction systems was analyzed by SEM (FEI Nova NanoSEM 230) [20]. Electron spin resonance (ESR, Bruker EMX plus-10/12, Germany) technology coupled with 5,5-dimethyl-1-pyrolin *N*-oxide (DMPO) as a spin trap was used to detect the free radical species [21].

3. Results and discussion

3.1. Enhanced effect of Fe^{2+} and Fe^{3+}

The effects of Fe^{2+} and Fe^{3+} on the enhanced removal of As(III) in PP-ZVI system are presented in Fig. 1. It can be seen that the removal rate of As(III) was close to 3% after 1 h in ZVI and PP-ZVI systems, which indicated that there was little change with the reaction proceeded. However, the release rate of Fe^{2+} was positively correlated with the removal rate of the specific pollutant [22], and the efficiency of As(III) removal was significantly improved by Fe^{2+}-PP-ZVI system (Fig. 1). Much to our surprise, the PP-ZVI system was activated by Fe^{2+} and achieved extremely high removal rate of As(III) in 0.5 min (Fig. 1). The role of Fe^{2+} in the reaction system might be an electron donor which could activate PP to produce $^{\bullet}OH$ [23], thus enhanced the activity of PP-ZVI system. Nevertheless, the removal efficiency of As(III) in Fe^{3+}-PP-ZVI system was even lower than that in Fe^{3+}-PP system within 30 min. Compared with the Fe^{3+}-PP system, the removal rate of As(III) in Fe^{3+}-PP-ZVI system was evidently enhanced and gradually approached to the 100% after 30 min (Fig. 1). The reason why As(III) in the Fe^{3+}-PP-ZVI system was rapidly removed after 30 min may be the reaction of ZVI with Fe^{3+} to form Fe^{2+}. So, it can

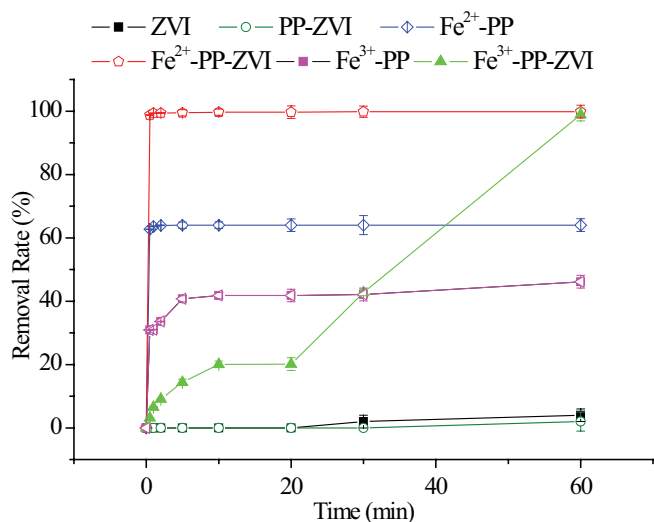Fig. 1. Comparison of the enhancement effects between Fe^{2+} and Fe^{3+} on the As(III) removal in PP-ZVI systems (initial concentration: 20 mg L^{-1} As(III), dosage of ZVI: 0.2 g, dosage of PP: 0.1 g, pH_{ini}: 7.0, temperature: 2°C).

be clearly concluded that the Fe^{3+} had an activation effect on the PP-ZVI system, but its activation ability was much weaker than that of Fe^{2+}.

3.2. Change of Fe^{2+} concentrations and pH values

To understand the phenomenon of Fig. 1, the Fe^{2+} concentrations and pH values in the reaction solution were monitored (Fig. 2). In Fe^{2+}-PP and Fe^{2+}-PP-ZVI systems, the Fe^{2+} concentrations dropped rapidly within 1 min (Fig. 2a), indicating that Fe^{2+} was consumed during the reaction process and Fe^{2+} could promote the reaction. It could be seen that the pH values of all reaction systems decreased rapidly within 0.5 min (Fig. 2b), which will promote the corrosion of ZVI and lead to increase the concentration of Fe^{2+} in

Fe^{2+}-PP-ZVI system after 30 min. Interestingly enough, the concentration of Fe^{2+} in Fe^{3+}-PP-ZVI system increased slowly within 30 min, while it increased significantly after 30 min (Fig. 2a). Meanwhile, the concentration of Fe^{2+} in Fe^{2+}-PP-ZVI system exceeded than that of Fe^{2+}-PP system after 30 min (Fig. 2a). Since ZVI was oxidized to Fe^{2+} by Fe^{3+} and corroded in the acidic solution, the concentration of Fe^{2+} was continuously enhanced in Fe^{3+}-PP-ZVI system. However, there was no ZVI producing Fe^{2+} continuously for the reaction in Fe^{2+}-PP system. ZVI continuously provided Fe^{2+} to the reaction and reacted with the oxidant, which successfully caused Fenton-like reactions to remove contaminants [24]. PP facilitated intensive corrosion of ZVI, promoting the surface of ZVI to become very rough and irregular, and producing Fe^{2+} [9]. The iron oxyhydroxides as the following production were responsible for effectively and quickly removing As(III). Other researchers also found the similar phenomenon [17]. It could be reasonably concluded that ZVI as an iron resource could be continuously provided Fe^{2+} as the activator for the systems. This result was consistent with the observation in Fig. 1.

3.3. Effects of Fe^{2+} and PP

In addition, we investigated the influence of Fe^{2+} and PP dosage on As(III) remediation in PP-ZVI system (Fig. 3). As shown in Fig. 3, with the amount of Fe^{2+} growing from 0.01g to 0.1 g, the removal rate of As(III) was enhanced from 51.32% to 99.99% at equilibrium condition in the system. Nevertheless, there was no obvious improvement of the removal ratio of As(III) in the solution when PP dosage was changed from 0.01 to 0.1 g with the same condition (Fig. 3). The addition of Fe^{2+} greatly activated the system and increased the As(III) removal percentage, so Fe^{2+} played a role in the activator for Fe^{2+}-PP-ZVI systems. On the contrary, the activity of the system was insignificantly improved as an increase of the dosage of PP, but the removal rate will be very relatively low if the ZVI system is completely devoid of PP. Therefore, it could be reckoned that Fe^{2+} accelerated
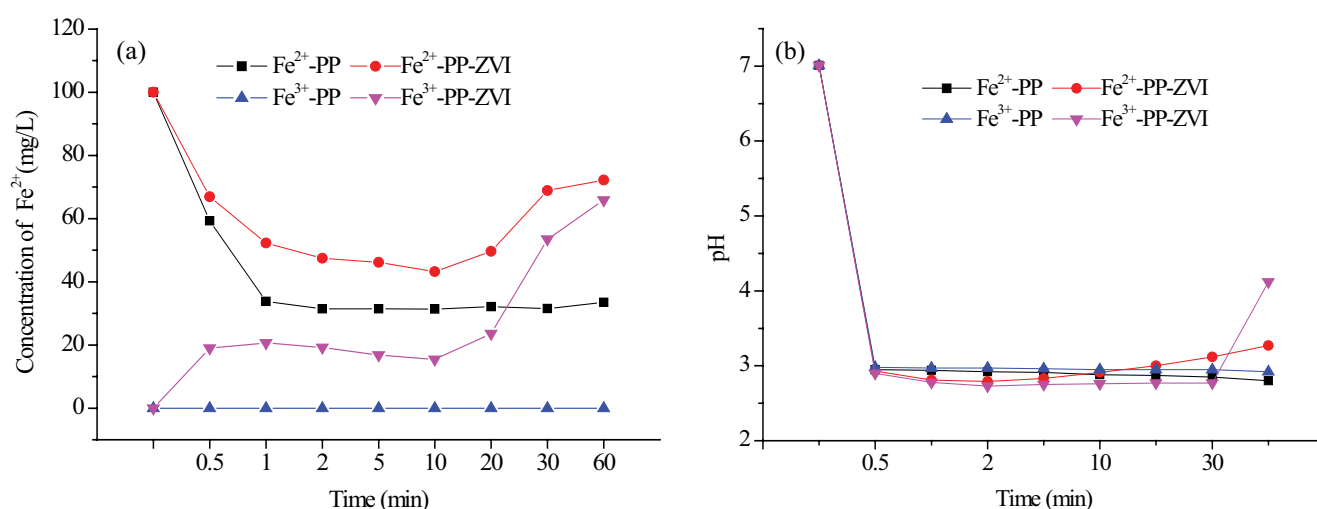

Fig. 2. Comparison of the change of Fe^{2+} concentrations (a) and pH values (b) in Fe^{2+}-PP-ZVI system (initial concentration: 20 mg L^{-1} As(III), dosage of ZVI: 0.2 g, dosage of PP: 0.1 g, pH_{ini}: 7.0, temperature: 20°C).
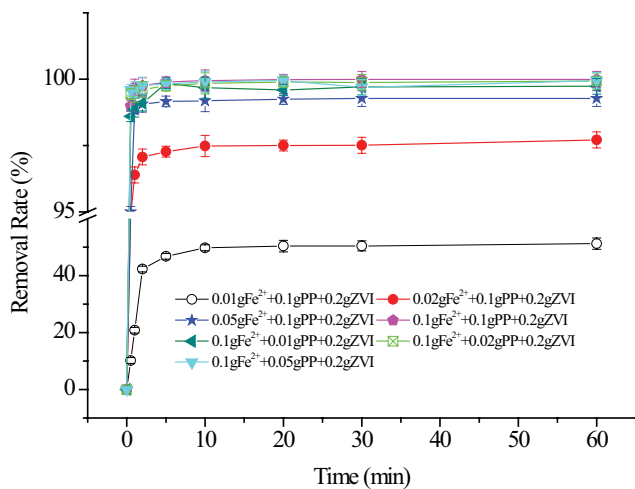
Fig. 3. Effect of Fe^{2+} and PP on the removal rates of As(III) (initial concentration: 20 mg L^{-1} As(III), the dosage of ZVI: 0.2 g, pH_{ini}: 7.0, temperature: 20°C).

Fig. 4. Effect of pH on the removal rates of As(III) in Fe^{2+}-PP-ZVI system (initial concentration: 20 mg L^{-1} As(III), dosage of ZVI: 0.2 g, dosage of PP: 0.1 g, pH_{ini}: 1.0, 3.0, 5.0, 7.0 and 9.0, temperature: 20°C).

and improved the removal rate of arsenic and PP was also an indispensable material for the system to remove arsenic from wastewater.

3.4. Effect of pH

The pH of the solution markedly affected the morphology of heavy metals and the surface active sites of the adsorbent [25]. The removal capacity of As(III) in Fe^{2+}-PP-ZVI system under different pH_{ini} is illustrated in Fig. 4. It can be seen that the removal ability of Fe^{2+}-PP-ZVI changed with varying pH value. When the initial pH was between 3.0 and 7.0, its influence on As(III) by Fe^{2+}-PP-ZVI was small, and the removal rate surpassed 99% at equilibrium (Fig. 4). As pH_{ini} 1, the removal rate was relatively low during the initial stage of reaction. In addition, it, that reached a balance, was close to 99.9% after 20 min (Fig. 4). As pH_{ini} 9, the final removal rate of the reaction was maintained at 94%, which was lower than that under acidic and neutral conditions (Fig. 4). These results indicated that the Fe^{2+}-PP-ZVI system could efficiently remove As(III) over pH range of 1.0–9.0. However, the lower removal ratio of As(III) in the Fe^{2+}-PP-ZVI system within 10 min at pH_{ini} 1.0 may be due to the very strong acid solution hindering the production of hydroxyl radical. According to this result, it could be reasonably speculated that the high removal efficiency of As(III) in Fe^{2+}-PP-ZVI system almost unlimited by pH.

3.5. Kinetics of As(III) removal

This research adopted the pseudo-first-order and pseudo-second-order kinetics model to investigate the removal of As(III) (20 mg L^{-1}) in Fe^{2+}-PP-ZVI system (Figs. 5 and S1). The fitting results showed that the correlation coefficient (R^2) of the pseudo-first-order was less than 0.81 (Fig. S1). However, the removal of As(III) by Fe^{2+}-PP-ZVI system conformed to the pseudo-second-order reaction kinetics because the R^2 value was more than 0.99 (Fig. 5). Furthermore, the fitting curves were generally identical, indicating that the
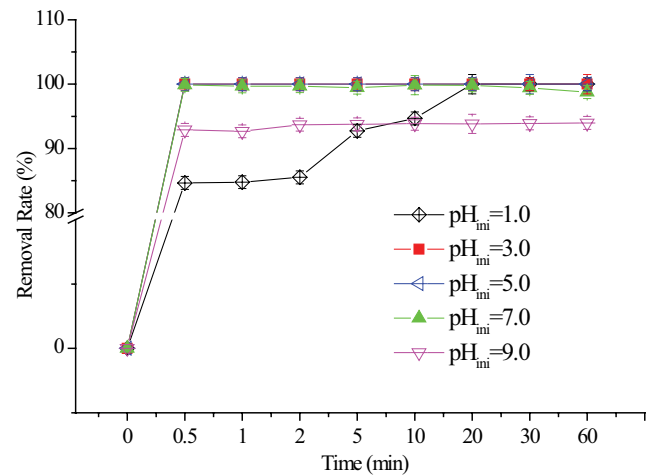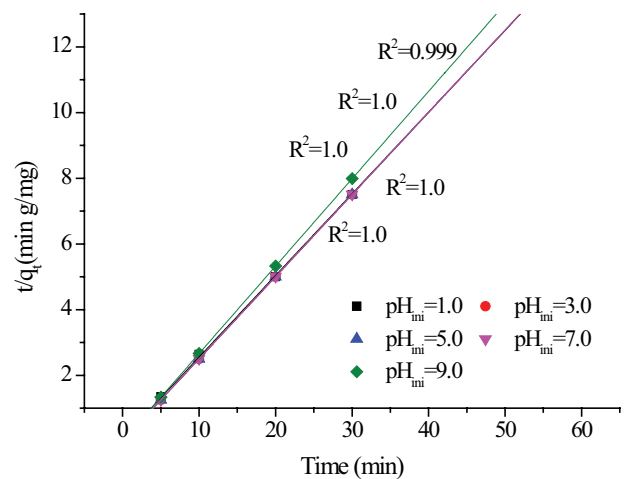

Fig. 5. Kinetics of As(III) adsorption in Fe^{2+}-PP-ZVI system. The reaction is pseudo-second-order with respect to the pH values. (Initial concentration: 20 mg L^{-1} As(III), dosage of ZVI: 0.2 g, dosage of PP: 0.1 g, pH_{ini}:1.0, 3.0, 5.0, 7.0 and 9.0, temperature: 20°C).

mechanism of removing As(III) in Fe^{2+}-PP-ZVI system was the same [20], that is, there was electron transfer or electron sharing between adsorbent and adsorbate. These comparisons revealed that pH significantly affected K_{obs}, but hardly affected the essence of removal in this system. Liu et al. [20] demonstrated that these two adsorption kinetic models could appropriately explain remediation of As(III) by nanoscale zero-valent iron supported on pumice. In this study, the process of As(III) removal might be accompanied by a complex removal mechanism in the Fe^{2+}-PP-ZVI system, so the removal process was hard to describe with the pseudo-first-order kinetics.

According to the pseudo-second-order reaction kinetics fitting results, the maximum adsorption capacity of As(III) in this system was 9.98 mg g^{-1}. Comparison of

arsenic removal by ZVI or iron oxide was shown in Table 1. The adsorbed amount of As(III) in groundwater was 1.2 mg As(III) g^{-1} ZVI [4]. The As(III) removal capacity of As(III) using NZVI was 3.5 mg g^{-1} [26]. The adsorption capacity of peerless Fe^0 for As(III) was about 1.771 mg g^{-1} [27]. The adsorption capacity of As(III) in our study was about 3–8 times that of other adsorbents. It was further proved that Fe^{2+}-PP-ZVI system had a higher adsorption capacity for As(III).

3.6. Morphological characterization

Fig. 6 shows the surface morphology of ZVI after being used. It was found that ZVI are agglomerated in a tight and dense form, and there were no visible adsorption sites on the surface of ZVI (Fig. 6a). Similarly, the surface of PP-ZVI remained almost unchanged and the degree of corrosion was still low (Fig. 6b). However, when Fe^{2+} was added into PP-ZVI system to remove As(III), the corrosion of ZVI was accelerated, and therefore significant changes occurred on the morphology of PP-ZVI (Figs. 6c and d). Sample surface became rough and formed many agglomerated particles, providing abundant active sites for the removal of contaminants (Figs. 6c and d). ZVI simply coupled with oxidants could rapidly and efficiently remove various heavy metals from wastewater through multiple mechanisms [17]. Due to ZVI surface corrosion, a great amount of iron oxides/hydroxides was continuously produced, which was essential for the removal of As(III) through oxidation, adsorption and co-precipitation [24]. The special morphology of ZVI in the Fe^{2+}-PP-ZVI system may indicate the multiple complex mechanism for the removal of As(III). This phenomenon was a strong positive evidence for the results in Fig. 1. The introduction of Fe^{2+} into PP-ZVI system accelerated the corrosion of ZVI and led to the rapid and effective removal of As(III).

3.7. Removal mechanisms of As(III)

The high resolution XPS spectra of Fe2p, Mn2p and As3d in Fe^{2+}-PP-ZVI system for As(III) removal at different reaction moments are shown in Fig. 7. There were two binding energy peaks at 711.6 and 725.2 eV (Fig. 7a), which matched with $2p_{3/2}$ and $2p_{1/2}$ of [Fe(III)] [28]. Furthermore, the peak of Fe^0 at around 706.7 eV did not appear in this study [28]. These features suggested that the iron particles surface coated with a layer of iron oxide/hydroxide film and little Fe^0 remained in 0.5 min. After 0.5 min, these peaks were enhanced and shifted to 710.0 and 723.6 eV (Figs. 7b and c), which meant that the oxidation of iron surface was continued and new stable iron(III) complexes were formed.
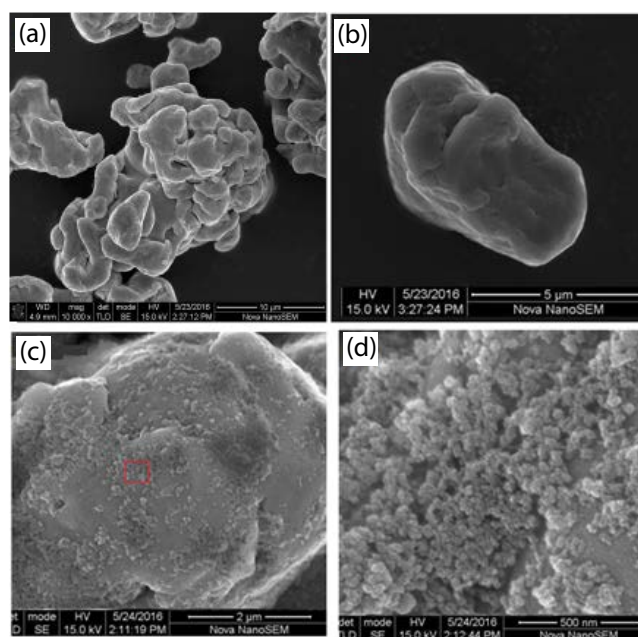

Fig. 6. Morphology of ZVI reacted with As(III) was analyzed: SEM image of (a) ZVI, (b) PP-ZVI, (c) Fe^{2+}-PP-ZVI, and (d) higher magnification of SEM image of Fe^{2+}-PP-ZVI marked with "□" in Fig. 6c.

Similarly, other studies showed that iron nanoparticles can be completely oxidized in 10 min [29,30].

The Mn2p spectrum showed four binding energy peaks at 653.9, 641.9, 651.9 and 640.6 eV (Fig. 7d). The peak at 653.9 and 641.9 eV can be ascribed to MnO_2, and the peak at 651.9 and 640.6 eV can be appointed to $MnFe_2O_4$ and MnO, respectively [31]. Then, after 1.0 min, characteristic peaks corresponding to MnO_2, $MnFe_2O_4$ and MnO were all suppressed and slightly shifted, however, a new peak at 644.1 eV was appeared (Fig. 7e). The new peak might be contributed to the new generation of Fe/Mn/As complex on the surface of ZVI. At 10 min, photoelectron peaks at 654.2 and 642.5 eV attributed to MnO_2 and 652.1 eV for $MnFe_2O_4$ were enhanced, otherwise, 641.0 eV for MnO was suppressed and the new peak at 640.4 eV assigned to MnO was appeared (Fig. 7f) [31]. Another new peak at 650.1 eV emerged (Fig. 7f), indicating that the reaction among iron/iron oxide, MnO_x and arsenic continued and produced new material. The finding might indicate that the reactive intermediates, $MnFe_2O_4$, MnO_2 and MnO, might be associated with the removal of As(III), through manipulating the

Table 1
Comparison of adsorption capacity of As(III) from wastewater by different adsorbent

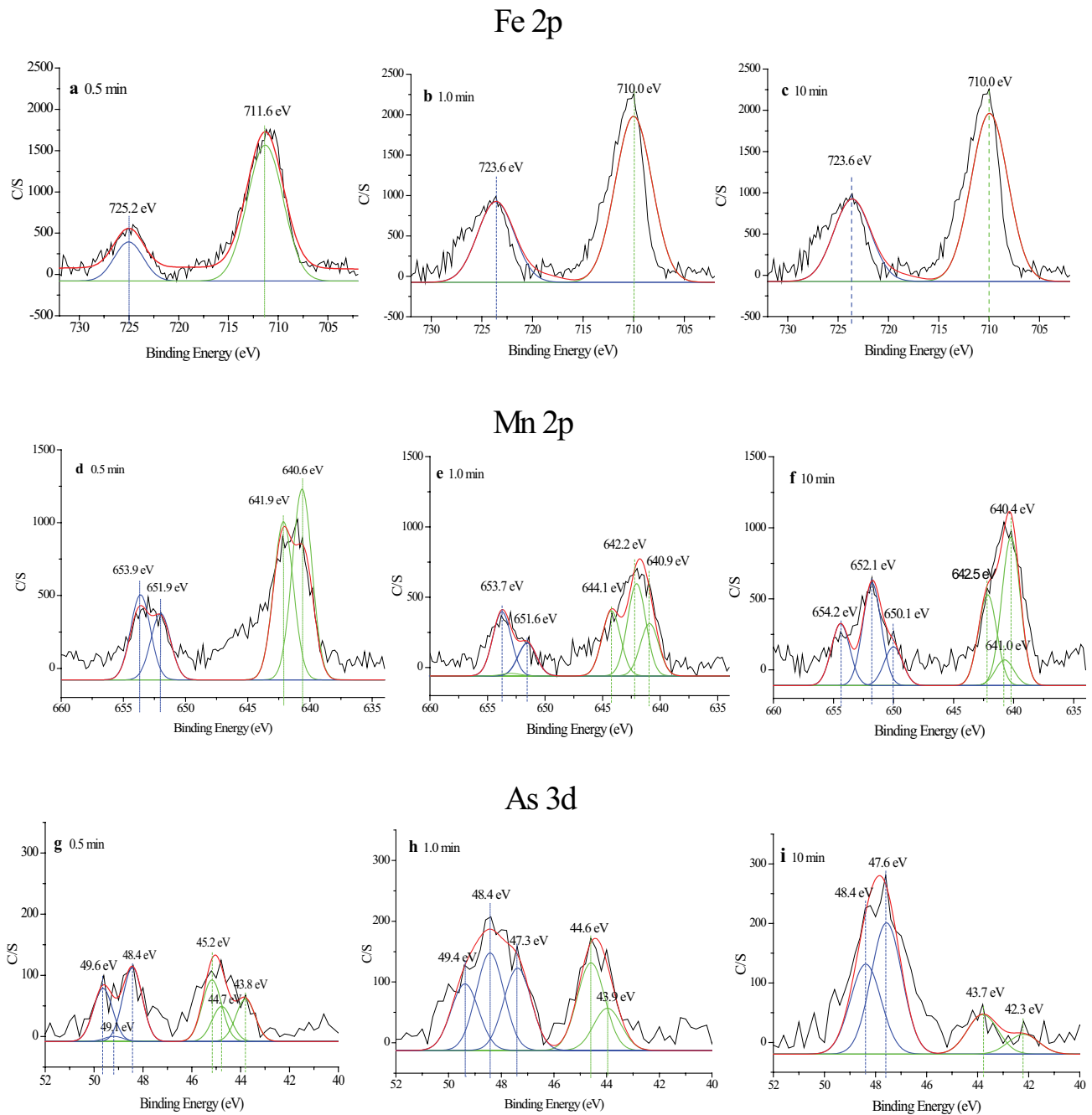| Type of adsorbent	Type of pollutants	Adsorption capacity (mg g^{-1})	References
ZVI	As(III)	1.2	[4]
NZVI	As(III)	3.5	[26]
Peerless Fe^0	As(III)	1.771 ± 0.032	[27]
Fe^{2+}-PP-ZVI	As(III)	9.98	Present study

Fe 2p

Mn 2p

As 3d

Fig. 7. High-resolution XPS survey of (a) Fe 2p, 0.5 min, (b) Fe 2p, 1.0 min, (c) Fe 2p, 10 min, (d) Mn 2p, 0.5 min, (e) Mn 2p, 1.0 min, (f) Mn 2p, 10 min, (g) As 3d, 0.5 min, (h) As 3d, 1.0 min and (i) As 3d, 10 min of Fe^{2+}-PP-ZVI at 10 min (initial concentration: 20 mg L^{-1} As(III), dosage of ZVI: 0.2 g, dosage of Fe^{2+}: 0.1 g, dosage of PP: 0.1 g, pH_{ini}: 7.0, temperature: 20°C).

generation of the hydroxyl radical (•OH) to enhance the rapid removal of the contaminant [15].

The XPS spectrum in the As3d region showed that the photoelectron peaks centered at 45.2 eV for As(V) and 44.7 and 43.8 eV for As(III) (Fig. 7g) [26,32]. The result suggested that the removal mechanism of As(III) included physical adsorption of As(III) as well as oxidization of As(III) to As(V) in Fe^{2+}-PP-ZVI system in 0.5 min. It was worth noting that three new peaks were formed at 49.6, 49.1 and 48.4 eV,

which might generate new complexes of iron, Mn and As. At 1.0 min, the peaks at 44.6 and 43.9 eV for As(III) became stronger (Fig. 7h) [26], suggesting that more As(III) was rapidly adsorbed by ZVI to the rugged surface. Interestingly, the peak at 45.2 eV for As(V) disappeared [32] and new peaks at 49.4, 48.4 and 47.3 eV were enhanced, hinting that more As(V) might be involved in the generation of complexes of iron, Mn and As. Then, the peaks of As(III) were enhanced and the peaks of As(V) were weaken, demonstrating more

As(III) was oxidized to As(V) after 1.0 min (Fig. 7i). A very small proportion of As(III) was reduced to As(0) because of a new peak corresponding to As(0) at 42.3 eV (Fig. 7i) [33]. Similar redox reactions occurred in arsenic in other systems [27,34]. In addition, As(III) was easily oxidized to As(V) when it approached or touched the ZVI surface [35]. The phenomenon is consistent with the result of Fig. 6.

Furthermore, in order to intensively study the mechanism, using ESR spectrometer combined with DMPO as a spin trap to directly detect free radicals at different reaction time intervals and the result is shown in Fig. 8. The hydroxyl radicals ($^\bullet$OH) and Fe(IV), produced in the Fenton-like reaction, could oxidize As(III) [34,36]. Wondrously, some scholars had found that As(III) was oxidized to As(IV) by $^\bullet$OH radicals as Eq. (1) [34]. Meanwhile, Fe(IV), an alternative strong oxidant species, was produced in the reaction, and could also produce transient species As(IV) as Eq. (2) [34]. As(IV), as an intermediate induced oxidation of As(III) by Fe(II)-H_2O_2 system, was readily oxidized to As(V) by oxygen [37].
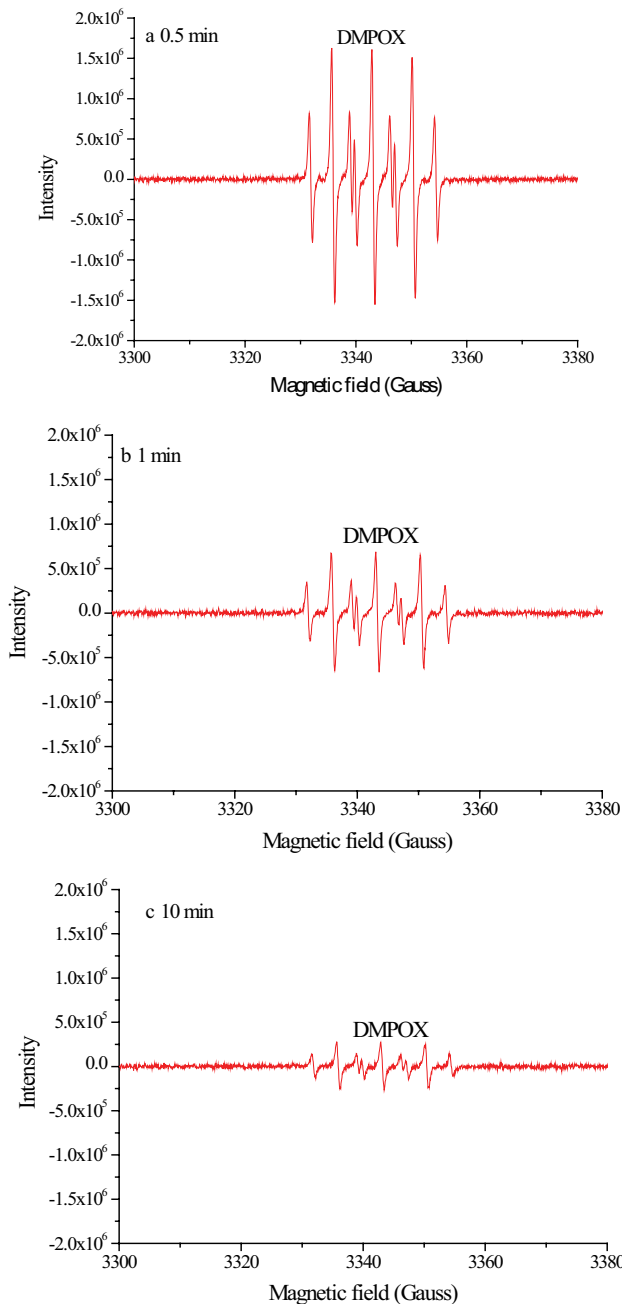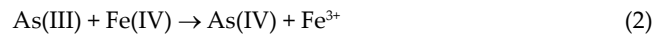
$$As(III) + {}^\bullet OH \rightarrow As(IV) \tag{1}$$

$$As(III) + Fe(IV) \rightarrow As(IV) + Fe^{3+} \tag{2}$$

However, $^\bullet$OH radicals are not found in Fig. 8. Interestingly, a new peak was formed in our study (Fig. 8), which was contributed to DMPOX [21,38]. DMPOX might form in Fe^{2+}-PP-ZVI systems in the following ways: (1) $^\bullet$OH was captured by DMPO to generate DMPO-OH, and then it was oxidized to DMPOX by Fe^{2+}/ZVI with $MnFe_2O_4$, MnO_2 and MnO as the catalyst [39]. (2) DMPO was oxidized by MnO_4^- led to the formation of DMPO-OH, followed by dehydrogenation to produce DMPOX [21]. As shown in Fig. 8, the intensity of DMPOX gradually dropped, suggesting that adduct of DMPOX was consumed during the As(III) removal process.

Surprisingly, one phenomenon was found that PP-ZVI system without Fe^{2+} had a low removal rate of As(III) or As(V) and did not increase with the reaction time, while they could be removed quickly and efficiently by Fe^{2+}-PP-ZVI system (Fig. S2). There were not detected $^\bullet$OH radicals in PP-ZVI system in the study (data not shown), but Fe^{2+}-PP-ZVI system, indicating that $^\bullet$OH radicals played a dominant effect. Interestingly, As(V) removal was mostly completed within 0.5 min in Fe^{2+}-PP-ZVI system, however, As(III) removal rate was only 79.8 % in 0.5 min and 99.91 % in 1 min. In the process, $^\bullet$OH radicals concentration was rapidly decreased (Figs. 8a and b). The decrease of $^\bullet$OH

Fig. 8. ESR obtained spectra for Fe^{2+}-PP-ZVI system at pH_{ini} = 4.6 after reaction for (a) 0.5 min, (b) 1 min, and (c) 10 min.
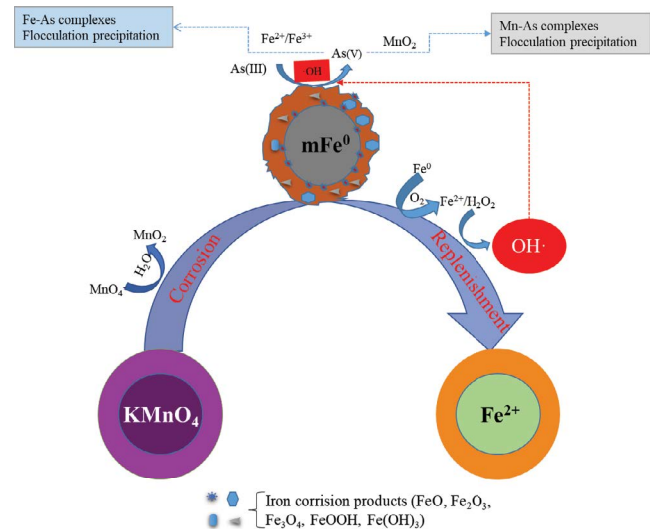

Fig. 9. Schematic diagram of the removal mechanism of As(III) by Fe^{2+}-PP-ZVI system.

radicals corresponded to the increase of As(V). A majority of As(III) were oxidized to As(V) before being removed in Fe^{2+}-PP-ZVI system.

Therefore, the results of Figs. 6–8 and S2 clearly supported the removal mechanism of As(III) using Fe^{2+}-PP-ZVI system given in a schematic model (Fig. 9). In addition, considering the recovery of zero-valent iron, we performed a magnetic separation experiment on ZVI. The results showed that the external magnetic field could quickly and efficiently separate ZVI from the solution (Fig. S3).

4. Conclusions

This study proved that As(III) could be quickly and efficiently removed from wastewater in Fe^{2+}-PP-ZVI system. ZVI as a resource sustainably provided Fe^{2+} as the activator for PP-ZVI system, which was rapidly activated by Fe^{2+} but Fe^{3+} in a slow way. The removal rate of As(III) in the Fe^{2+}-PP-ZVI system was always high in a large pH range of 1–9. The kinetic studies showed that the adsorption process of Fe^{2+}-PP-ZVI system to As(III) conformed to the pseudo-second-order model, and other researchers had similar findings [20]. In addition, the maximum adsorption capacity of the system for As(III) was 10 mg g^{-1}, which was much higher than the previous work that the adsorption capacity of ZVI and NZVI for As(III) was 1.2 and 3.5 mg g^{-1}, respectively [4,26]. The results of XPS, ESR proved that the intermediate products $MnFe_2O_4$, MnO_2 and MnO enhanced the removal of As(III) by manipulating the generation of the hydroxyl radical ($^\bullet$OH). Lot of As(III) was oxidized to As(V) by $^\bullet$OH before being adsorbed and a very small portion of As(III) was reduced to As(0) by ZVI. The main mechanism was adsorption, which can form complexes of iron, Mn, As on the ZVI surface. Furthermore, the Fe^{2+}-PP-ZVI system, as an economical technology, is obviously beneficial to remediate As(III) in the field of in situ and provided potential value to remove other pollutions from the water.

References

[1] M. Deng, X.D. Wu, A.M. Zhu, Q.G. Zhang, Q.L. Liu, Well-dispersed TiO_2 nanoparticles anchored on Fe_3O_4 magnetic nanosheets for efficient arsenic removal, J. Environ. Manage., 237 (2019) 63–74.

[2] Y.N. Chen, C.S. Xiong, Adsorptive removal of As(III) ions from water using spent grain modified by polyacrylamide, J. Environ. Sci., 45 (2016) 124–130.

[3] Y. Yu, L. Yu, K.Y. Koh, C.H. Wang, J.P. Chen, Rare-earth metal based adsorbents for effective removal of arsenic from water: a critical review, Crit. Rev. Env. Sci. Technol., 48 (2018) 1127–1164.

[4] D.L. Wu, Y. Zong, Z.Y. Tian, B.B. Shao, Role of reactive oxygen species in As(III) oxidation by carbonate structural Fe(II): a surface-mediated pathway, Chem. Eng. J., 368 (2019) 980–987.

[5] Y.X. Deng, Y.T. Li, X.J. Li, Y. Sun, J. Ma, M. Lei, L.P. Weng, Influence of calcium and phosphate on pH dependency of arsenite and arsenate adsorption to goethite, Chemosphere, 119 (2018) 617–624.

[6] R. Sridar, U.U. Ramanane, M. Rajasimman, Synthesis, characterization of ZVI nanoparticles and its application for the removal of phenol from wastewater, Desal. Wat. Treat., 122 (2018) 42–49.

[7] A.A.H. Faisal, T.R. Abbas, S.H. Jassam, Removal of zinc from contaminated groundwater by zero-valent iron permeable reactive barrier, Desal. Wat. Treat., 55 (2015) 1586–1597.

[8] M. Gil-Diaz, J. Alonso, E. Rodríguez-Valdés, J.R. Gallego, M.C. Lobo, Comparing different commercial zero valent iron nanoparticles to immobilize As and Hg in brownfield soil, Sci. Total Environ., 584 (2017) 1324–1332.

[9] X.J. Guo, Z. Yang, H. Liu, X.F. Lv, Q.S. Tu, Q.D. Ren, X.H. Xia, C.Y. Jing, Common oxidants activate the reactivity of zero-valent iron (ZVI) and hence remarkably enhance nitrate reduction from water, Sep. Purif. Technol., 146 (2015) 227–234.

[10] L. Xu, Y.H. Huang, Kinetics and mechanism of selenite reduction by zero valent iron under anaerobic condition activated and enhanced by dissolved Fe(II), Sci. Total Environ., 664 (2019) 698–706.

[11] P. Drzewicz, L. Perez-Estrada, A. Alpatova, J.W. Martin, M.G. El-Din, Impact of peroxydisulfate in the presence of zero valent iron on the oxidation of cyclohexanoic acid and naphthenic acids from oil sands process-affected water, Environ. Sci. Technol., 46 (2012) 8984–8991.

[12] J.S. Du, B. Sun, J. Zhang, X.H. Guan, Parabola-like shaped pH-rate profile for phenols oxidation by aqueous permanganate, Environ. Sci. Technol., 46 (2012) 8860–8867.

[13] M.R. Samaei, H. Maleknia, A. Azhdarpoor, A comparative study of removal of methyl tertiary-butyl ether (MTBE) from aquatic environments through advanced oxidation methods of H_2O_2/nZVI, H_2O_2/nZVI/ultrasound, and H_2O_2/nZVI/UV, Desal. Wat. Treat., 57 (2016) 21417–21427.

[14] M. Tong, S.H. Yuan, P. Zhang, P. Liao, A.N. Alshawabkeh, X.J. Xie, Y.X. Wang, Electrochemically induced oxidative precipitation of Fe(II) for As(III) oxidation and removal in synthetic groundwater, Environ. Sci. Technol., 48 (2014) 5145–5153.

[15] B. Sun, X.H. Guan, J.Y. Fang, P.G. Tratnyek, Activation of manganese oxidants with bisulfite for enhanced oxidation of organic contaminants: the involvement of Mn(III), Environ. Sci. Technol., 49 (2015) 12414–12421.

[16] G. Han, C. Wei, Permanganate with a double-edge role in photodegradation of sulfamethoxazole: kinetic, reaction mechanism and toxicity, Chemosphere, 191 (2018) 494–502.

[17] X.J. Guo, Z. Yang, H.Y. Dong, X.H. Guan, Q.D. Ren, X.F. Lv, X. Jin, Simple combination of oxidants with zero-valent-iron (ZVI) achieved very rapid and highly efficient removal of heavy metals from water, Water Res., 88 (2016) 671–680.

[18] Z. Wang, J. Jiang, S.Y. Pang, Y. Zhou, C.T. Guan, Y. Gao, J. Li, Y. Yang, W. Qiu, C.C. Jiang, Is sulfate radical really generated from peroxydisulfate activated by iron(II) for environmental decontamination?, Environ. Sci. Technol., 52 (2018) 11276–11284.

[19] Z.L. Chen, K.F. Akter, M.M. Rahman, R. Naidu, The separation of arsenic species in soils and plant tissues by anion-exchange chromatography with inductively coupled mass spectrometry using various mobile phases, Microchem. J., 89 (2008) 20–28.

[20] T.Y. Liu, Y.L. Yang, Z.-L. Wang, Y.Q. Sun, Remediation of arsenic(III) from aqueous solutions using improved nanoscale zero-valent iron on pumice, Chem. Eng. J., 288 (2016) 739–744.

[21] K. Xu, W.W. Ben, W.C. Ling, Y. Zhang, J.H. Qu, Z.M. Qiang, Impact of humic acid on the degradation of levofloxacin by aqueous permanganate: kinetics and mechanism, Water Res., 123 (2017) 67–74.

[22] J.X. Li, H.J. Qin, X.H Guan, Premagnetization for enhancing the reactivity of multiple zero-valent iron samples toward various contaminants, Environ. Sci. Technol., 49 (2015) 14401–14408.

[23] X.L. Shi, N.S. Dalal, V. Vallyathan, ESR evidence for the hydroxyl radical formation in aqueous suspension of quartz particles and its possible significance to lipid peroxidation in silicosis, J. Toxicol. Environ. Health, 25 (1988) 237–245.

[24] Y.-G. Kang, H. Yoon, W. Lee, E.-J. Kim, Y.-S. Chang, Comparative study of peroxide oxidants activated by nZVI: removal of 1,4-dioxane and arsenic(III) in contaminated waters, Chem. Eng. J., 334 (2018) 2511–2519.

[25] G. Crini, H.N. Peindy, F. Gimbert, C. Robert, Removal of C.I. Basic Green 4 (Malachite Green) from aqueous solutions by adsorption using cyclodextrin-based adsorbent: kinetic and equilibrium studies, Sep. Purif. Technol., 53 (2007) 97–110.

[26] S.R. Kanel, B. Manning, L. Charlet, H. Choi, Removal of arsenic (III) from groundwater by nanoscale zero-valent iron, Environ. Sci. Technol., 39 (2005) 1291–1298.

[27] L. Ling, W.-x. Zhang, Visualizing arsenate reactions and encapsulation in a single zero-valent iron nanoparticle, Environ. Sci. Technol., 51 (2017) 2288–2294.

[28] X.Y. Huang, L. Ling, W.X. Zhang, Nanoencapsulation of hexavalent chromium with nanoscale zero-valent iron: high resolution chemical mapping of the passivation layer, J. Environ. Sci., 67 (2018) 4–13.

[29] T.Y. Liu, Z.L. Wang, L. Zhao, X. Yang, Enhanced chitosan/Fe⁰-nanoparticles beads for hexavalent chromium removal from wastewater, Chem. Eng. J., 189–190 (2012) 196–202.

[30] T.Y. Liu, X. Yang, Z.L. Wang, X.X. Yan, Enhanced chitosan beads-supported Fe⁰-nanoparticles for removal of heavy metals from electroplating wastewater in permeable reactive barriers, Water Res., 47 (2013) 6691–6700.

[31] E. Beyreuther, S. Grafström, L.M. Eng, C. Thiele, K. Dörr, XPS investigation of Mn valence in lanthanum manganite thin films under variation of oxygen content, Phys. Rev., 73 (2006) 155425.

[32] S.R. Kanel, J.-M. Grenèche, H. Choi, Arsenic(V) removal from groundwater using nanoscale zero-valent iron as a colloidal reactive barrier material, Environ. Sci. Technol., 40 (2006) 2045–2050.

[33] C. Su, R.W. Puls, Arsenate and arsenite removal by zerovalent iron: kinetics, redox transformation, and implications for in situ groundwater remediation, Environ. Sci. Technol., 35 (2001) 1487–1492.

[34] S.J. Hug, O. Leupin, Iron-catalyzed oxidation of arsenic(III) by oxygen and by hydrogen peroxide: pH-dependent formation of oxidants in the Fenton reaction, Environ. Sci. Technol., 37 (2003) 2734–2742.

[35] J. Farrell, J.P. Wang, P. O'Day, M. Conklin, Electrochemical and spectroscopic study of arsenate removal from water using zero-valent iron media, Environ. Sci. Technol., 35 (2001) 2026–2032.

[36] I.A. Katsoyiannis, T. Ruettimann, S.J. Hug, Response to "comment on 'pH dependence of Fenton reagent generation and As(III) oxidation and removal by corrosion of zero valent iron in aerated water'", Environ. Sci. Technol., 43 (2009) 3980–3981.

[37] R. Woods, I.M. Kolthoff, E.J. Meehan, Arsenic (IV) as an intermediate in the induced oxidation of As (III) by the iron (II)-hydrogen peroxide reaction, J. Am. Chem. Soc., 86 (1964) 1698–1700.

[38] G.D. Mao, P.D. Thomas, M.J. Poznansky, Oxidation of spin trap 5,5-dimethyl-1-pyrroline-1-oxide in an electron paramagnetic resonance study of the reaction of methemoglobin with hydrogen peroxide, Free Radical Biol. Med., 16 (1994) 493–500.

[39] W.D. Zhang, C. Wang, Z.J. Li, Z.Z. Lu, Y.Y. Li, J.-J. Yin, Y.-T. Zhou, X.F. Gao, Y. Fang, G.J. Nie, Y.L. Zhao, Unraveling stress-induced toxicity properties of graphene oxide and the underlying mechanism, Adv. Mater., 24 (2012) 5391–5397.
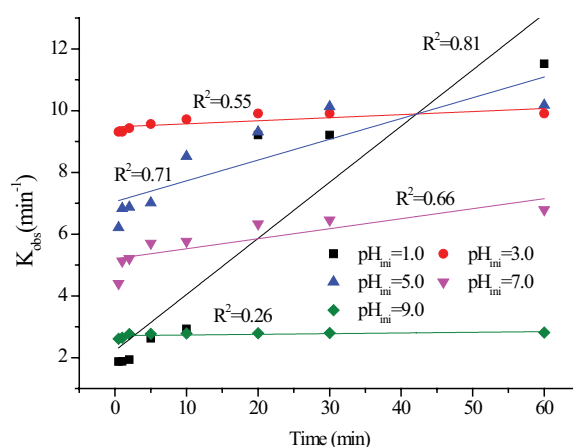
Supplementary Information

Fig. S1. Kinetics of As(III) adsorption in Fe^{2+}-PP-ZVI system. The reaction is not pseudo-first-order with respect to the pH values.
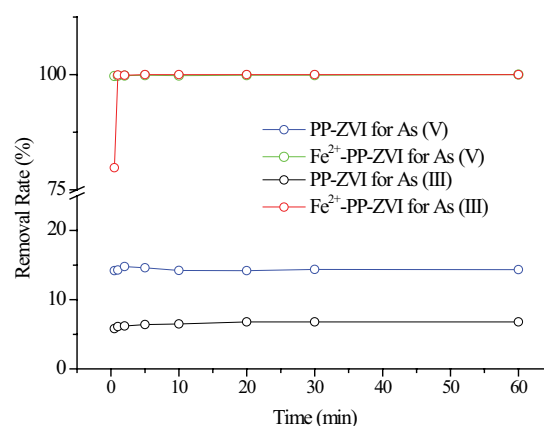

Fig. S2. Comparison of the removal efficiency of As(III) and As(V) using PP-ZVI and Fe^{2+}-PP-ZVI (initial concentration: 20 mg L^{-1} As(III) or As(V), dosage of ZVI: 0.2 g, dosage of Fe^{2+}: 0.1 g, dosage of PP: 0.1 g, pH_{ini}: 5.0, temperature: 20°C).
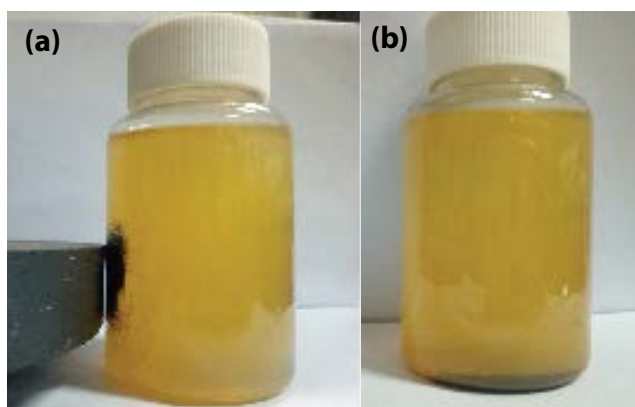

Fig. S3. Separation of ZVI using a magnet (a) and no external magnet (b).